Experimental and Molecular Pathology 110 (2019) 104274

Contents lists available at ScienceDirect

Experimental and Molecular Pathology

journal homepage: www.elsevier.com/locate/yexmp

Characteristics of liver fibrosis associated with chronic *Opisthorchis felineus* infection in Syrian hamsters and humans

Anna V. Kovner[a,*], Maria Y. Pakharukova[a,b,c], Galina A. Maksimova[a], Viatcheslav A. Mordvinov[a]

[a] Institute of Cytology and Genetics, Siberian Branch of Russian Academy of Sciences, Prospekt Lavrentyeva 10, Novosibirsk 630090, Russia
[b] Novosibirsk State University, Pirogova str., 1, Novosibirsk 630090, Russia
[c] Institute of Molecular Biology and Biophysics, Akademika Timakova str., 2, Novosibirsk 630117, Russia

ARTICLE INFO

Keywords:
O. Felineus
Fibrosis
Syrian hamster
Human
Cholecystitis

ABSTRACT

The food-borne liver trematode *Opisthorchis felineus* causes severe liver damage, including fibrosis. This study shows a comparison of the characteristics between cholangiofibrosis and periductal fibrosis in infected people and in the golden hamster as an experimental model. Comparative evaluation was carried out regarding collagen composition, the number of basic-producing cells, and extracellular-matrix degradation. The results revealed that characteristics of chronic opisthorchiasis due to *O. felineus* infection in humans and in Syrian hamsters are similar and include well-pronounced development of fibrotic complications in the liver parenchyma. Besides, a difference in fibrogenesis development was demonstrated between chronic *O. felineus* infection and non-infectious cholecystitis. In this study, we for the first time compared fibrogenesis between humans and model animals against the background of chronic *O. felineus* infection.

1. Introduction

The number of people with foodborne trematodiasis exceeds 40 million according to the WHO. Among the causative agents of this disease, the family of Opisthorchiidae occupies a special place. *Opisthorchis felineus*, *Opisthorchis viverrini*, and *Clonorchis sinensis* are epidemiologically significant representatives of the Opisthorchiidae family. *O. felineus* is distributed in the regions from Eastern Europe to Central Asia with the largest habitats in Western Siberia (Pakharukova and Mordvinov, 2016). Currently, the IARC classifies *O. viverrini* and *C. sinensis* as first-order carcinogens that initiate the development of cholangiocarcinoma (IARC, 2012). On the other hand, *O. felineus* is considered only a third-order carcinogen (IARC, 2012). Nonetheless, a similar manifestation of helminthiasis caused by the above trematodes was observed (Gouveia et al., 2017; Maksimova et al., 2017).

Opisthorchiasis associated with *O. felineus* may cause damage to the organs of the hepatobiliary system, including such conditions as cholangitis, cholecystitis, liver abscess, egg-granulomas, hyperplasia, metaplasia and dysplasia of cholangiocytes, hepatitis, and fibrosis (Sripa et al., 2007; Mairiang et al., 2012; Maksimova et al., 2017). Due to the imposed chronic mechanical damage and secretion of the excretory–secretory product, *O. felineus* promotes the development of i) periductal fibrosis, manifested in the excessive deposition of extracellular matrix (ECM) components in large bile ducts, and ii) cholangiofibrosis, i.e., excessive deposition of ECM proteins in the region of small bile ducts of portal triads (Brazhnikova and Tskhai, 2004; Maksimova et al., 2017). A massive fibrosis area can often be visualized in opisthorchis-associated cholangiocarcinoma (Chamadol et al., 2014; Maksimova et al., 2017). Unfortunately, treatment of chronic opisthorchiasis does not reduce the extent of fibrotic complications in the liver (Charoensuk et al., 2016).

The development of liver fibrosis provokes significant morbidity and mortality in humans (Gäbele et al., 2003). In this regard, there exists a major demand for the development of therapeutic strategies to counteract fibrosis progression (Baiocchini et al., 2016). A prerequisite for designing such strategies is ample knowledge of the ECM state. Preventing fibrotic lesions after opisthorchiasis treatment is a promising strategy to alleviate this opisthorchiasis-associated complication, including cholangiocarcinoma (Charoensuk et al., 2016). In this vein, the key factor for preventing fibrosis is ample knowledge of the ECM state. Infection-induced mechanical and toxic damage causes a permanent imbalance in the ECM, thus leading to fibrosis (Adhyatmika et al., 2015). Specifically, the normal ECM amount is supported by two main enzymes: matrix metalloproteinases (MMPs) and tissue inhibitors

Abbreviations: ECM, extracellular matrix; MMPs, matrix metalloproteinases; TIMPs, tissue inhibitors of matrix metalloproteinases; TGFβ1, transforming growth factor; α-SMA, α-smooth muscle actin; FSP, fibroblast surface protein; GFAP, glial fibrillary acidic protein; HSCs, hepatic stellate cells; p.i., post infection

* Corresponding author.
E-mail addresses: anya.kovner@gmail.com (A.V. Kovner), pmaria@yandex.ru (M.Y. Pakharukova), mordvin@bionet.nsc.ru (V.A. Mordvinov).

https://doi.org/10.1016/j.yexmp.2019.104274
Received 29 November 2018; Received in revised form 11 February 2019
Available online 19 June 2019

of matrix metalloproteinases (TIMPs). Imbalanced concentration of either of these proteins could be responsible for the progression of fibrosis in the affected organ (Schuppan et al., 2018). This imbalance leads to the deposition of "bad collagens of fibrosis": collagens, whose population increases as fibrosis progresses and that perform central structural and profibrotic signaling functions in the diseased organ, such as type I and III collagens and excess type IV collagen in the basement membrane (Karsdal et al., 2017). Thus, a systematic study of collagen data in *O. felineus* chronic opisthorchiasis should help to select the best targeted antifibrotic therapy.

All things considered, characterizing the fibrogenesis of the liver during chronic opisthorchiasis caused by *O. felineus* is of major importance for preventing opisthorchiasis-associated complications in humans. This study was aimed at bridging this gap through experiments on fibrogenesis in the liver of i) humans and ii) Syrian hamsters.

2. Materials and methods

2.1. Ethical statement

The procedures were in compliance with The Code of Ethics of the World Medical Association (Declaration of Helsinki) for animal experiments (http://ec.europa.eu/environment/chemicals/lab_animals/legislation_en.htm). Syrian hamsters (*Mesocricetus auratus*) were purchased from the stock of the Puschino Animal Facility (Russia) and bred at the Animal Facility of the ICG SB RAS (RFMEFI61914X0005) (Russia). The hamsters were maintained according to protocols approved by the Committee on the Ethics of Animal Experiments of the Institute of Cytology and Genetics (Permission Number: 25 of 12.12.2014).

The Ethics Committee of the Institute of Molecular Biology and Biophysics approved the analysis of human samples (Protocol #2/2016 of 27.10.2016). All the participants provided written informed consent. Participants ranged in age from 40 to 81 years. Liver samples were collected from the liver fractions captured during cholecystectomy in i) people infected with *O. felineus* ($n = 10$), and ii) people with cholecystitis, not associated with parasitic infestation ($n = 2$). The infection in the former group was confirmed by the analysis of blood samples (ELISA, antibody detection, Vector-BEST, Russia) and IHC using anti-*O. felineus* GST and anti-Tpx specific antiserum (Pakharukova et al., 2017; Petrenko et al., 2017) (data not shown). Thus, the infection was detected for the first time, patients had not been tested for the presence of eggs in feces and, consiquently, they had not been received anthelminthic therapy. The disease was most likely due to the consumption of undercooked fish, since all patients had a long history of eating this sort of fish, and it was not possible to determine the duration of infection.

The samples were collected during therapeutic intervention for cholelithiasis involving laparoscopic cholecystectomy performed at the 2nd Novosibirsk City Hospital, Novosibirsk, Russia. During cholecystectomy, the samples were dispensed into a sterile tube with 10% formaldehyde and dispatched immediately to the laboratory.

2.2. Parasites, hamsters, and experimental design

Metacercariae of *O. felineus* were collected from naturally infected *Leuciscus idus* from the Ob River, Novosibirsk city, Western Siberia, and isolated from muscle tissues through digestion with pepsin–HCl overnight at 37 °C. The fish were collected from neither conservation areas nor private property and were not otherwise protected; hence, fishing permits were not required. *Leuciscus idus* is not considered endangered or rare, and the fishing methods complied with the Federal Law N166-F3 of 20.12.2004 (ed. 18.07.2011) "Fishing and conservation of water bio-resources" (Maksimova et al., 2017; Gouveia et al., 2017).

Male Syrian hamsters aged 6–8 weeks were orally infected with 50 *O. felineus* metacercariae. The rodents were housed at three to four individuals per cage under conventional conditions and received a stock diet and water ad libitum. Control non-infected hamsters ($n = 6$) and *O. felineus*-infected hamsters (n = 6) were euthanized using carbon dioxide and necropsied 30 weeks post infection (p.i.).

2.3. Sample collection

In humans, samples of the gallbladder along with the liver, were fixed in a 10% aqueous solution of neutral formalin and were dehydrated in a graded series of ethanol and in xylene (STP-120, Thermo Scientific). Dehydrated samples were enclosed in a paraffinic medium HISTOMIX (BioVitrum). For microscopic examination, sections of 3.5 μm thickness were prepared on a rotary microtome Microm HM 355S (Thermo Scientific). In Syrian hamsters, tissue samples were taken from the large right lobe of the liver and were subjected to similar chemical processing.

2.4. Histopathology and immunohistochemistry

The resulting paraffin sections were stained via a standard protocol with hematoxylin and eosin, Van Gieson picrofuxin (detecting connective tissue fibers), Ag^+ staining (detection of "young" argyrophilic fibers of connective tissue). To determine the phenotype of effector cells, typing and assessment of collagen ECM were carried out with the immunohistochemical kit (SpringBioScience kit HRP-125) using specific primary antibodies:

1) against collagens: collagen I (Abcam, cat. # ab34710, 1:200), collagen III (Abcam, ab7778, 1:100), collagen IV (Abcam, ab6586, 1:50);
2) against the fibrosis regulation system: transforming growth factor (TGFβ1; Abcam, ab92486, 1:200), α-smooth muscle actin (α-SMA; Abcam, ab7817, 1:300), MMP2 (SpringBioScience, E18014, 1:100), MMP9 (Abcam, ab58803, 1:100), TIMP1 (Abcam, ab216432, 1:100);
3) against effector cell markers: fibroblast surface protein FSP (Abcam, ab11333, 1:300), glial fibrillary acidic protein (GFAP) from hepatic stellate cells (HSCs) (Abcam, ab7260, 1:300).

Staining was performed according to the manufacturer's protocol. The visualization was carried out under an AxioImager A1 microscope (Zeiss) with camera AxioCam MRc (Zeiss).

Because of the size and location of the collection of liver samples from humans, only random sections of the parenchyma were available for evaluation and comparison with the experimental group. In this regard, in human samples, only cholangiofibrosis could be analyzed. To assess the state of cholangiofibrosis in hamsters and in humans, 20 random visual fields of parenchyma were used. In Syrian hamsters, we also evaluated periductal fibrosis in 10 visual fields in the hepatic large bile duct in a closed test system $3.6 \times 10^5\ \mu m^2$ per 100 points. Semiquantitative analysis was carried out with the following scoring of the results for the volume density of fibrosis: "0," 0–5%; "1," 5–10%; "2," 10–15%; "3," 15–20%; "4," > 20%. For the numerical density of cells: "0," 0–20; "1," 20–40; "2," 40–60; "3," 60–80; "4," > 80.

2.5. RT-PCR

The total RNA was isolated using the AxyPrep Multisource Total RNA Miniprep Kit (Axygen Biosciences, USA). DNA was treated with DNase I, RNase-free (Fermentas, USA). For cDNA synthesis, we used the High Capacity cDNA Archive Kit (Applied Biosystems, USA). The expression levels of genes *Tgfβ1* and *Gapdh* were determined by real-time PCR in the presence of SYBR Green I (Syntol, Russia) on an ABI PRISM 7000 (Thermo Fisher Scientific, USA). The expression levels of genes *Acta2* and *Hprt1* were determined by real-time PCR in the presence of EVA Green (Syntol, Russia) on a CFX96 real-time PCR system (Bio-Rad, USA). The primer sequences were as follows: transforming growth

factor Tgfβ1 F (5′-CCAACTATTGCTTCAGCTCCAC-3′); Tgfβ1 R (5′-CAGGGCCAGGACCTTGCT-3′); glyceraldehyde 3-phosphate dehydrogenase Gapdh F (5′-GAACATCATCCCTGCATCCACT-3′); Gapdh R (5′-ATGCCTGCTTCACCACCTTCTT-3′); hypoxanthine phosphoribosyltransferase Hprt1 F (5′-TCCTTAGTCAAGCGGTACAAC-3′); Hprt1 R (5′-ATCTGGCCTATATCCAACACTTC-3′); and α smooth muscle actin Acta2 F (5′- GGATGCAGAAGGAGATCACAG-3′); Acta2 R (5′-TGGAAG GTAGACAGAGACGC-3′); Acta2 R (5′-R6G-TTCATGGTGCTGGGTGCG AGA-BHQ2) (Syntol, Russia) The expression of the *Tgfβ1* gene was normalized to the expression of the *Gapdh* gene, and the level of expression of the *Acta2* gene to *Hprt1*.

2.6. Statistical analysis

The resulting quantitative RT-PCR data were statistically analyzed in the Statistica 6.0 software (Statsoft, USA). Significance of the differences between the experimental groups was assessed by the Mann–Whitney *U* test. Data with *P* values $\leq .05$ were considered significant.

3. Results

3.1. Hamster samples

In a histopathological analysis of the liver tissue of Syrian hamsters, at 30 weeks p.i., *O. felineus* manifested forceful development of fibrotic complications, both in the parenchyma (cholangiofibrosis) and around the large bile ducts (periductal fibrosis; Fig. 1). In the control group, the presence of cholangiofibrosis and periductal fibrosis was not detected. In infected animals, the composition of connective tissue, regardless of the site of its localization, revealed the presence of young argyrophilic reticulin fibers. This result indicated dynamic development of organ fibrosis. The percentage of young argyrophilic reticulin fibers in the connective tissue predominated in the cholangiofibrosis zones (Fig. 2). In control animals, stand-alone young fibers were detected in the sinusoids; this finding is consistent with the norm.

In untreated Syrian hamsters, type I, III, and IV collagens were identified individually in the portal triad and liver sinusoids in the analysis of collagen composition of the ECM. *O. felineus*–infected animals had significant areas of collagen deposition and slight differences between periductal fibrosis and cholangiofibrosis. In periductal fibrosis, the predominance of type I and IV collagen was registered, and type I collagen prevailed in the parenchymal region (Figs. 1 and 2).

The number of cells classically responsible for fibrogenesis in the liver—fibroblasts (FSP–positive cells) and activated HSCs [GFAP-positive cells (Hassan et al., 2014)]—slightly different from that in the control group (Fig. 2).

Examination of the expression of key fibrogenic genes showed significant upregulation of TGF-β1 in the group of infected hamsters, and no difference between the two groups in terms of the α-SMA gene expression (Supplementary Fig. 1). Nevertheless, at the protein level, chronic opisthorchiasis in Syrian hamsters was characterized by a slight increase in the number of cells expressing the TGF-β1 marker and increasing α-SMA deposition relative to the animals in the control group (Figs. 1 and 2).

The absence of fibrotic complications in the control group can be caused not only by the absence of effector cells of fibrogenesis but also by the correct balance of the ECM regulation system. In the control group, MMP-2 and -9 versus TIMP-1 were in the correct balance, approximately 1:1 (Figs. 1 and 2). In contrast, disruption of the balance between matrix metalloproteinases and their tissue inhibitor was detected in infected hamsters, in favor of TIMP-1 (Figs. 1 and 2).

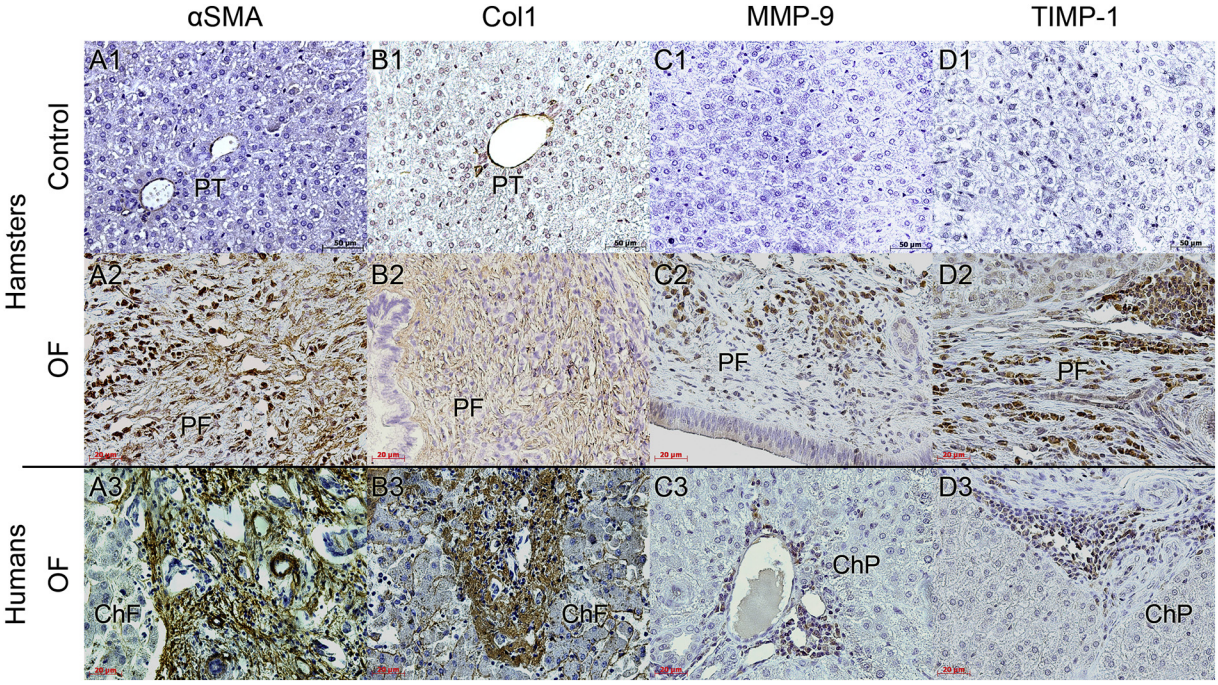

Fig. 1. Representative histological picture of the features of liver fibrogenesis of Syrian hamsters (A1-D1; A2-D2) and human samples (A3-D3), immunohistochemical analysis. A. α-SMA. A1. Control: a lack of positive staining. Magnification × 200. A2. OF hamster: a high degree of periductal fibrosis positive for α-SMA. Magnification × 400. A3. OF human: a high degree of cholangiofibrosis positive for α-SMA, formation of false lobules. Magnification × 400. B. Type I collagen (Col I). B1. Control: minimal deposition of type I collagen in the portal tract area. Magnification × 100. B2. OF hamster: a high degree of cholangiofibrosis positive for type I collagen. Magnification × 400. B3. OF human: scale deposition zone of type I collagen. Magnification × 400. C. MMP-9. C1. Control: stand-alone positive cells. Magnification × 200. C2. OF hamster: accumulation of staining-positive cells. Magnification × 400. C3. OF human: accumulation of staining-positive cells. Magnification × 400. D. TIMP-1. D1. Control: stand-alone positive cells. Magnification × 200. D2. OF hamster: massive accumulation of staining-positive cells. Magnification × 400. D3. OF human: well-pronounced accumulation of staining-positive cells. Magnification × 400.

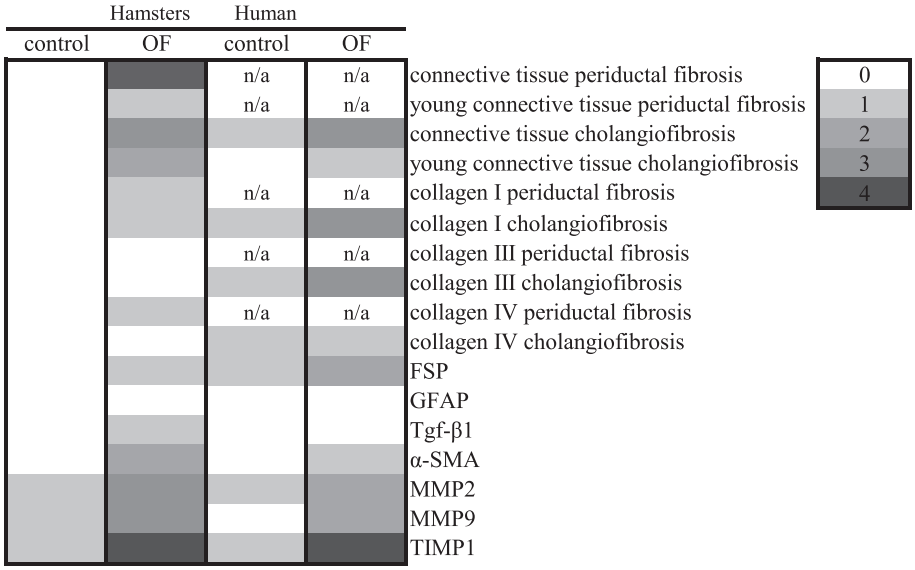

Fig. 2. A heat map of fibrotic changes in the liver tissue of Syrian hamsters and humans. Note: n/a: not possible to determine due to the specific nature of the obtained samples, PF: periductal fibrosis, ChF: cholangiofibrosis.

3.2. Human samples

In the liver samples of patients infected with *O. felineus*, indirectly, the presence of a chronic inflammation might be seen by histopathology. The presence of large-scale cholangiofibrosis areas, proliferation of small bile ducts, common loci of granular dystrophy of hepatocytes and the absence of eosinophils in the inflammatory infiltrate.

In humans with clinically confirmed chronic presence of *O. felineus* invasion and in humans with cholecystitis, we detected the presence of cholangiofibrosis. Among the features of fibrosis during chronic opisthorchiasis, it is possible to identify a greater number of large-scale zones of cholangiofibrosis with a tendency to form false liver lobules. In addition, the presence of young argyrophilic reticulin fibers in the connective tissue was detected in contrast to people with chronic cholecystitis; this finding is evidence of a more dynamic process during *O. felineus* infection (Figs. 1 and 2, Supplementary Fig. 2).

Between the two comparable groups of humans, there were differences in the types of collagen in the liver parenchyma ECM. In humans with chronic opisthorchiasis, large-scale predominant deposition of type I and III collagens was detected (Fig. 1). In the group of people with chronic cholecystitis, there was slight deposition of all three types of collagens under study (Fig. 2).

In this regard, the number of activated fibroblasts was also greater in the group of humans with chronic opisthorchiasis. It should be noted that there were single activated GFAP-positive HSCs and TGF-β1–positive liver cells in both comparison groups. In the group of humans with chronic opisthorchiasis, in contrast to humans with cholecystitis, a small amount of α-SMA protein in the cholangiofibrosis zone was also detectable (Figs. 1 and 2).

Differences in the system regulating deposition of ECM proteins were detected in both comparison groups. In the group of humans with chronic opisthorchiasis, the same amounts of MMP-2 and MMP-9 were detected, with predominance and imbalance toward TIMP-1. In the group of humans with cholecystitis, TIMP-1 also predominated, with almost complete absence of MMP-9 (Fig. 2).

4. Discussion

Characteristics of chronic opisthorchiasis associated with *O. felineus* infection are similar between humans and Syrian hamsters and include well-pronounced development of fibrotic complications in the liver parenchyma. We also demonstrated for the first time deposition of argyrophilic reticulin fibers in the periductal area and cholangiofibrosis at the stage of chronic opisthorchiasis, both in humans and in hamsters. These data indicate progressive unstable fibrosis and are consistent with the data on the deposition of reticulin fibers in the liver in patients with chronic infections by *Schistosoma mansoni* (de Oliveira et al., 2017).

In this study, the features of liver fibrogenesis—that was caused by chronic *O. felineus* exposure in Syrian hamsters—are similar to the pathological changes reported in studies on *O. viverrini* infection. Thus, the same tendency is observed: the predominance of type I collagen over all other types of collagens (Prakobwong et al., 2009; Khoontawad et al., 2012; Charoensuk et al., 2016). We chose to analyze these three types of collagen (types I, III, and IV) because of their greatest significance in fibrosis processes (Thompson et al., 2011). Excessive deposition of type I collagen is associated with the progression of fibrotic complications (Karsdal et al., 2017).

TGF-β1 is one of the central genes of fibrogenesis and regulates deposition of type I collagen. We demonstrated an increase in both the protein and mRNA expression of TGF-β1 in Syrian hamsters during chronic opisthorchiasis. Currently, when comparing the level of TGF-β1 mRNA in the liver of animals infected with *O. felineus* (7.5 month p.i.) and *O. viverrini* (6 month p.i.), our data is more consistent with the research of Pinlaor et al., 2010 (untreated infected hamsters) (Pinlaor et al., 2010). Increasing expression of TGF-β1 results in a proportional increase in the expression of the α-SMA gene, during chronic infection with *O. felineus* or with *O. viverrini* (Charoensuk et al., 2016). It should be noted that among the collagen-producing cells, FSP fibroblasts and stand-alone activated stellate cells (HSCs) predominated. In contrast, *Fasciola hepatica* infection promotes the development of liver fibrosis by activating the HSCs (Machicado et al., 2016).

The main reason for the progression of fibrosis is the imbalance of MMPs and TIMPs in the ECM regulation system (Duarte et al., 2015). Previously, the elevated MMP-2 and MMP-9 mRNA levels in the liver of Syrian hamsters infected with *O. viverrini* was shown, while TIMP-1 mRNA levels exceeded both control values and metalloproteinase values (Prakobwong et al., 2009). At the protein level, the authors detected MMP-9 predominance over MMP-2.

In our study, we detected the predominance of TIMP-1 over MMP-2 and -9; probably as a consequence, collagen deposits predominantly involve types I and III.

The comparison of fibrogenesis in humans between chronic *O. felineus* infection and cholecystitis uncovered some differences. In chronic opisthorchiasis, there was a larger area of deposition of type I and III collagens, which increased the number of activated fibroblasts, and accordingly, there was a larger amount of α-SMA protein. Probably due to the difference in the amount of collagen deposited in the ECM, the balance of matrix metalloproteinases and their tissue inhibitor was different. In humans with chronic cholecystitis, there is virtually no MMP-9 and weakly expressed MMP-2, resulting in the same deposition of all types of collagen (Duarte et al., 2015).

As a result, we registered predominance of type I collagen among ECM proteins and FSP fibroblasts as the main fibroblast effector cells during chronic *O. felineus* infection. In the future, these data will allow for an additional targeted therapy for opisthorchiasis. At present, there are significant successes in the downregulation of type I collagen and restoration of the balance in the ECM regulation system by phytochemicals and antioxidants (Pinlaor et al., 2010; Xu et al., 2013; Charoensuk et al., 2016).

Nevertheless, since patients did not undergo intraoperative ultrasound to show exact location of the infection, we have to admit that we might have not got enough information about inflammation and fibrosis.

5. Conclusion

The fibrogenesis associated with infection by *O. felineus*—despite its wide range of habitats and clinical significance—has not been studied enough, in contrast to other trematodes. In our study, we for the first time compare fibrogenesis in humans and model animals (*M. auratus*) during chronic *O. felineus* infection. A similar picture of cholangiofibrosis of the liver in humans and Syrian hamsters confirms the suitability of the latter as an experimental model of opisthorchiasis. Liver fibrogenesis in Syrian hamsters has common features between chronic infections with *O. felineus* and *O. viverrini*; this result confirms similarity of the effects of these helminthiases. To compare the characteristics of liver fibrogenesis between infections by various trematodes, further studies of fibrosis associated with *O. felineus* infection at different stages of the disease are needed.

Supplementary data to this article can be found online at https://doi.org/10.1016/j.yexmp.2019.104274.

Funding

This work was supported by the Russian Science Foundation grant No. 18-15-00098.

Declarations of interest

None.

Declaration of Competing Interest

The authors declare that they have no conflicts of interest.

References

Adhyatmika, A., Putri, K.S., Beljaars, L., Melgert, B.N., 2015. The elusive antifibrotic macrophage. Front. Med. (Lausanne). 2, 81. https://doi.org/10.3389/fmed.2015.00081.

Baiocchini, A., Montaldo, C., Conigliaro, A., et al., 2016. Extracellular matrix molecular remodeling in human liver fibrosis evolution. PLoS One 11, e0151736. https://doi.org/10.1371/journal.pone.0151736.

Brazhnikova, N.A., Tskhai, V.F., 2004. Clinic, diagnosis and treatment of complications of opisthorchiasis. Ann. Surg. Hepatol. 9, 92–99.

Chamadol, N., Pairojkul, C., Khuntikeo, N., Laopaiboon, V., Loilome, W., Sithithaworn, P., Yongvanit, P., 2014. Histological confirmation of periductal fibrosis from ultrasound diagnosis in cholangiocarcinoma patients. J. Hepatobiliary Pancreat. Sci. 21, 316–322. https://doi.org/10.1002/jhbp.64.

Charoensuk, L., Pinlaor, P., Wanichwecharungruang, S., Intuyod, K., Vaeteewoottacharn, K., Chaidee, A., Yongvanit, P., Pairojkul, C., Suwannateep, N., Pinlaor, S., 2016. Nanoencapsulated curcumin and praziquantel treatment reduces periductal fibrosis and attenuates bile canalicular abnormalities in *Opisthorchis viverrini*-infected hamsters. Nanomedicine. 12, 21–32. https://doi.org/10.1016/j.nano.2015.10.005.

de Oliveira, F.L., Carneiro, K., Brito, J.M., et al., 2017. Galectin-3, histone deacetylases, and hedgehog signaling: possible convergent targets in schistosomiasis-induced liver fibrosis. PLoS Negl. Trop. Dis. 11, e0005137. https://doi.org/10.1371/journal.pntd.0005137.

Duarte, S., Baber, J., Fujii, T., Coito, A.J., 2015. Matrix metalloproteinases in liver injury, repair and fibrosis. Matrix Biol. 44-46, 147–156. https://doi.org/10.1016/j.matbio.2015.01.004.

Gäbele, E., Brenner, D.A., Rippe, R.A., 2003. Liver fibrosis: signals leading to the amplification of the fibrogenic hepatic stellate cell. Front. Biosci. 8, 69–77.

Gouveia, M.J., Pakharukova, M.Y., Laha, T., et al., 2017. Infection with *Opisthorchis felineus* induces intraepithelial neoplasia of the biliary tract in a rodent model. Carcinogenesis. 38, 929–937. https://doi.org/10.1093/carcin/bgx042.

Hassan, S., Syed, S., Kehar, S.I., 2014. Glial fibrillary acidic protein (GFAP) as a mesenchymal marker of early hepatic stellate cells activation in liver fibrosis in chronic hepatitis C infection. Pak. J. Med. Sci. 30 (5), 1027–1032. https://doi.org/10.12669/pjms.305.5534.

IARC Working Group on the Evaluation of Carcinogenic Risks to Humans, 2012. Biological agents. Volume 100 B. a review of human carcinogens. IARC Monogr. Eval. Carcinog. Risks Hum. 100, 1–441.

Karsdal, M.A., Nielsen, S.H., Leeming, D.J., et al., 2017. The good and the bad collagens of fibrosis - their role in signaling and organ function. Adv. Drug Deliv. Rev. 121, 43–56. https://doi.org/10.1016/j.addr.2017.07.014.

Khoontawad, J., Laothong, U., Roytrakul, S., et al., 2012. Proteomic identification of plasma protein tyrosine phosphatase alpha and fibronectin associated with liver fluke, *Opisthorchis viverrini*, infection. PLoS One 7, e45460. https://doi.org/10.1371/journal.pone.0045460.

Machicado, C., Machicado, J.D., Maco, V., Terashima, A., Marcos, L.A., 2016. Association of *Fasciola hepatica* infection with liver fibrosis, cirrhosis and cancer: a systematic review. PLoS Negl. Trop. Dis. 10, e0004962. https://doi.org/10.1371/journal.pntd.0004962.

Mairiang, E., Laha, T., Bethony, J.M., et al., 2012. Ultrasonography assessment of hepatobiliary abnormalities in 3,359 subjects with *Opisthorchis viverrini* infection in endemic areas of Thailand. Parasitol. Int. 61, 208–211. https://doi.org/10.1016/j.parint.2011.07.009.

Maksimova, G.A., Pakharukova, M.Y., Kashina, E.V., Zhukova, N.A., Kovner, A.V., Lvova, M.N., Mordvinov, V.A., 2017. Effect of *Opisthorchis felineus* infection and dimethylnitrosamine administration on the induction of cholangiocarcinoma in Syrian hamsters. Parasitol. Int. 66, 458–463. https://doi.org/10.1016/j.parint.2015.10.002.

Pakharukova, M.Y., Mordvinov, V.A., 2016. The liver fluke *Opisthorchis felineus*: biology, epidemiology and carcinogenic potential. Trans. R. Soc. Trop. Med. Hyg. 110, 28–36. https://doi.org/10.1093/trstmh/trv085.

Pakharukova, M.Y., Kovner, A.V., Trigolubov, A.N., Fedin, E.N., Mikhailova, E.S., Shtofin, S.G., Autenshlyus, A.I., Mordvinov, V.A., 2017. Mechanisms of trematodiases pathogenicity: the presence of the secretory proteins from the liver fluke *Opisthorchis felineus* in the gallbladder tissues of the patients with chronic opisthorchiasis. Vavilov J. Genet. Breed. 21 (3), 312–316. https://doi.org/10.18699/VJ16.17-o.

Petrenko, V.A., Pakharukova, M.Y., Kovner, A.V., L'vova, M.N., Mordvinov, V.A., Lyakhovich, V.V., 2017. Secretion of thioredoxin peroxidase protein of cat liver fluke *Opisthorchis felineus* during modeling of experimental opisthorchiasis. Bull. Exp. Biol. Med. 162 (6), 773–776. https://doi.org/10.1007/s10517-017-3710-5.

Pinlaor, S., Prakobwong, S., Hiraku, Y., Pinlaor, P., Laothong, U., Yongvanit, P., 2010. Reduction of periductal fibrosis in liver fluke-infected hamsters after long-term curcumin treatment. Eur. J. Pharmacol. 638 (1–3), 134–141. d. https://doi.org/10.1016/j.ejphar.2010.04.018.

Prakobwong, S., Pinlaor, S., Yongvanit, P., Sithithaworn, P., Pairojkul, C., Hiraku, Y., 2009. Time profiles of the expression of metalloproteinases, tissue inhibitors of metalloproteases, cytokines and collagens in hamsters infected with *Opisthorchis viverrini* with special reference to peribiliary fibrosis and liver injury. Int. J. Parasitol. 39, 825–835. https://doi.org/10.1016/j.ijpara.2008.12.002.

Schuppan, D., Ashfaq-Khan, M., Yang, A.T., Kim, Y.O., 2018. Liver fibrosis: direct antifibrotic agents and targeted therapies. Matrix Biol. 68-69, 435–451. https://doi.org/10.1016/j.matbio.2018.04.006.

Sripa, B., Kaewkes, S., Sithithaworn, P., et al., 2007. Liver fluke induces cholangiocarcinoma. PLoS Med. 4, e201. https://doi.org/10.1371/journal.pmed.0040201.

Thompson, K.J., McKillop, I.H., Schrum, L.W., 2011. Targeting collagen expression in alcoholic liver disease. World J. Gastroenterol. 17, 2473–2481. https://doi.org/10.3748/wjg.v17.i20.2473.

Xu, L., Zheng, N., He, Q., Li, R., Zhang, K., Liang, T., 2013. Puerarin, isolated from Pueraria lobata (Willd.), protects against hepatotoxicity via specific inhibition of the TGF-β1/Smad signaling pathway, thereby leading to anti-fibrotic effect. Phytomedicine. 20, 1172–1179. https://doi.org/10.1016/j.phymed.2013.06.008.